Inkjet-Printed Nanocavities on a Photonic Crystal Template

Frederic S. F. Brossard, Vincenzo Pecunia,* Andrew J. Ramsay, Jonathan P. Griffiths, Maxime Hugues, and Henning Sirringhaus*

The last decade has witnessed the rapid development of inkjet printing as an attractive bottom-up microfabrication technology due to its simplicity and potentially low cost. The wealth of printable materials has been key to its widespread adoption in organic optoelectronics and biotechnology. However, its implementation in nanophotonics has so far been limited by the coarse resolution of conventional inkjet-printing methods. In addition, the low refractive index of organic materials prevents the use of "soft-photonics" in applications where strong light confinement is required. This study introduces a hybrid approach for creating and fine tuning high-*Q* nanocavities, involving the local deposition of an organic ink on the surface of an inorganic 2D photonic crystal template using a commercially available high-resolution inkjet printer. The controllability of this approach is demonstrated by tuning the resonance of the printed nanocavities by the number of printer passes and by the fabrication of photonic crystal molecules with controllable splitting. The versatility of this method is evidenced by the realization of nanocavities obtained by surface deposition on a blank photonic crystal. A new method for a free-form, high-density, material-independent, and high-throughput fabrication technique is thus established with a manifold of opportunities in photonic applications.

Compact 2D photonic crystal (PhC) devices based on high-refractive-index inorganic semiconductors such as silicon and GaAs have been widely explored for a range of applications. In particular, photonic crystal cavities have the highest finesse of any photonic nanocavity, lending themselves to applications in strong-coupling,[1–3] single photon sources,[4,5] low threshold lasers,[6,7] and sensing.[8–11] Recently, deep UV photolithography has been successfully employed for the fabrication of high quality PhC cavities,[12,13] thus paving the way for their mass production. Concurrently, a few reports have emerged on the possibility of creating nanocavities by depositing a low-refractive-index polymer on a photonic crystal waveguide.[14–17] This is suggestive of the technological and scientific potential that could be realized by bringing patterned unconventional low-refractive-index materials into intimate contact with conventional inorganic PhC templates: on the one hand, the production of photonic devices by postprocessing a generic, mass-produced, photonic crystal template; on the other hand, new device architecture/functionalities and fundamental light–matter interaction studies through the wealth of solution-processable nano-, hybrid, and soft materials that have emerged over the last decade. However, this potential has been frustrated thus far, as the approaches pursued to date for the deposition of the low-refractive-index materials relied on e-beam or UV exposure technique, both being highly material specific and requiring multiple complex fabrication steps.

Here we propose and demonstrate the printing of nanocavities using an electrohydrodynamic jet printer with femtoliter droplet delivery[18–20] on a generic 2D photonic crystal template. Our free-form, bottom-up approach offers the possibility of assigning by design any solution processable material on the surface of a photonic crystal in a single fabrication step. In the following, we demonstrate the fine tuning of the cavity emission and the reproducible printing of nanocavities with high *Q* factors, which also enable the fabrication of photonic molecules with controllable splitting. Three different cavity designs are

Dr. F. S. F. Brossard, Dr. A. J. Ramsay
Hitachi Cambridge Laboratory
Cavendish Laboratory
J J Thomson Avenue
Cambridge CB3 0HE, UK
E-mail: fsfb2@cam.ac.uk

Dr. V. Pecunia, J. P. Griffiths, Prof. H. Sirringhaus
Cavendish Laboratory
University of Cambridge
J J Thomson Avenue
Cambridge CB3 0HE, UK
E-mail: vp293@cam.ac.uk

DOI: 10.1002/adma.201704425

Dr. V. Pecunia
Institute of Functional Nano & Soft Materials (FUNSOM)
Jiangsu Key Laboratory for Carbon-Based Functional Materials & Devices
Soochow University
199 Ren'ai Road, Suzhou 215123 Jiangsu, P. R. China

Dr. M. Hugues
Department of Electronic and Electrical Engineering
University of Sheffield
Mapping Street, Sheffield S1 3JD, UK

Dr. M. Hugues
Universite Cote d'Azur
CRHEA-CNRS
Sophia Antipolis
Rue Bernard Gregory
06560 Valbonne, France

explored. We use both a PhC template with a waveguide line-defect, and a blank PhC template to illustrate the free-form nature of our approach. We compare cavities made by drawing a strip, and by depositing a single droplet of ink. Thus a new fabrication method is established, where nanophotonic devices are printed on generic, Original Equipment Manufacturer, "OEM," photonic crystal templates.

A schematic of the nanocavities fabrication method using a commercially available electrohydrodynamic[21] high-resolution inkjet printer[19] is shown in **Figure 1**A. Droplets are ejected on demand by applying a voltage between the ink reservoir (i.e., the nozzle) and the sample substrate. The PhC template, which consists of photonic crystal membranes suspended in air (see Experimental Section), is mounted on a programmable stage enabling the deposition of ink droplets with micrometer accuracy. The selected nozzle (orifice feature size of about 1 μm) and the applied voltage waveform allow the ejection of droplets with volume in the 1–10 fL range, a method that we refer to as femtoliter inkjet printing in the following (FlIJ printing). While the deposition method is material independent, in the experiments reported below we employed an organic ink consisting of a mixture of a small molecule (a spirooxazine) and a polymer (poly(methyl methacrylate)), denoted as SPO:PMMA in the following, dissolved in dichlorobenzene.

We found that the femtoliter droplet volume is essential for the printed material to remain on and cover the assigned region of the PhC membranes. In fact, larger ink droplets, as obtained with nozzle orifices in the 5–10 μm range, undergo immediate dewetting to the side of the PhC membranes. By contrast, femtoliter droplets give reliable structures covering the PhC membrane regions assigned by design. This is consistent with their much higher surface-to-volume ratio and consequent enhancement of drying rate and viscosity. The printed structures on the PhC membranes, taking the form of strips and disks depending on design, are characterized by lateral feature size of ≈1 μm, consistent with the estimated droplet diameter. As expected from an additive solution-based process, their thickness can be controlled by varying the ink solid content, and fine-tuned via the number of overlaid printing passes as shown in the inset of Figure 1A. The voltage waveform and printing speed offer further levers. By varying these parameters, we achieve SPO:PMMA structures on the PhC membranes with thicknesses ranging from a few nanometers to fractions of a micrometer. For thickness values below 50 nm, the cross-sectional profile of the printed structures presented a corrugation reproducing the underlying membranes, with valleys corresponding to the air holes. For thicker structures, a smooth profile was observed, as shown in the AFM map of Figure 1B. Remarkably, the FlIJ-printed structures on the PhC templates presented a convex profile, a near-perfect truncated Gaussian in the case of printed strips. Therefore, we did not observe the coffee ring effect which results from the capillary flow taking

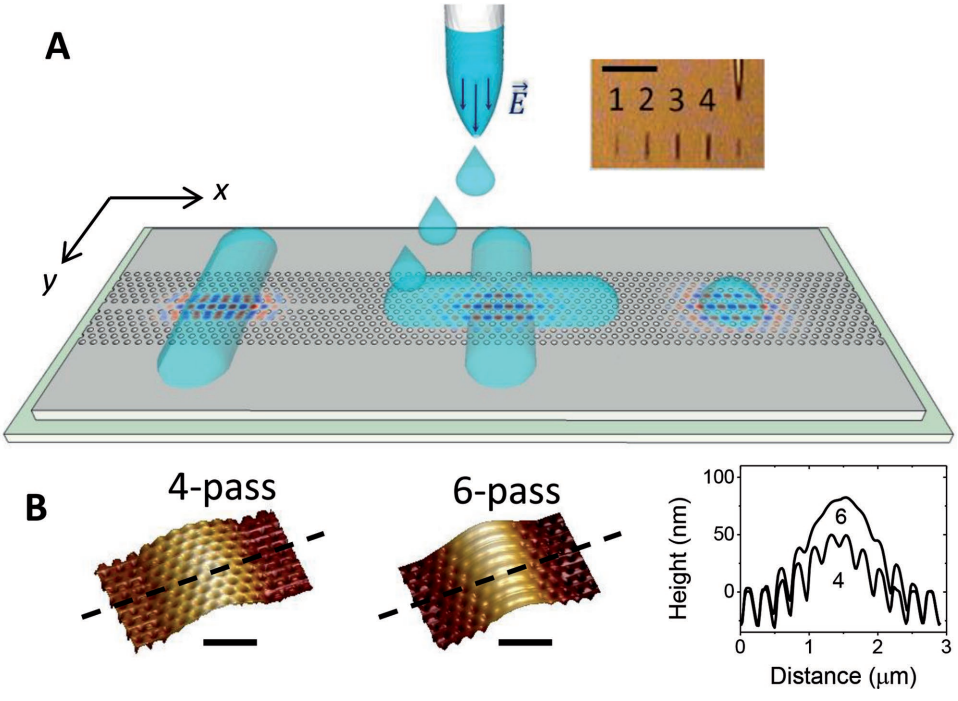

Figure 1. FlIJ printing on a PhC template for the patterning of nanocavities. A) Schematic illustration of the patterning process by deposition of an organic compound on the surface of a PhC template with a high resolution electrohydrodynamic inkjet printer. The printed structures investigated in this work include strips on a PhC waveguide (left) and intersecting strips and standalone dots on a blank PhC (middle and right). Overlaid are their respective calculated *Ey* electric field distribution, which relate to their functionality as nanocavities detailed in subsequent figures. Inset: Optical micrograph showing the inkjet printing of SPO:PMMA strips with increasing number of overlaid passes from 1 to 4. The distance between the printer nozzle shown on the right to the sample surface was about 50 μm (scale bar 100 μm). B) AFM images of a printed strip on the surface of a PhC with four and six overlaid printer passes (scale bar 1 μm). The cross-sectional height profile of each strip along the dashed lines is shown on the right. The printed strips present a corrugation at low thickness, with valleys corresponding to the air-holes of the PhC.

place during the droplet drying process.[22–24] This is in spite of the relatively high-boiling-point solvent adopted, which further substantiates the rapid drying allowed by FlIJ printing.

The applicability of FlIJ printing to hybrid nanophotonics was first investigated in combination with a PhC waveguide template. The PhCs used in these experiments were obtained from a GaAs wafer comprising quantum dot (QD) emitters for photoluminescence (PL) mapping. A GaAs substrate with embedded QDs was chosen purely for convenience, i.e., for ease of characterization of the cavities and coupled-cavity systems demonstrated in this work. The patterning method using inkjet printing shown here is directly applicable to a silicon substrate or any other high-refractive-index substrate, which can be processed to form a photonic crystal template. The device consists of an organic strip printed across the waveguide, as shown in **Figure 2**A. This particular design is attractive for its simplicity and insensitivity to misalignment. The strip increases the average refractive index of the PhC lattice at the intersection with the PhC waveguide, providing lateral confinement for the waveguide modes to form an optical cavity.[14] The creation of a nanocavity by inkjet printing is unambiguously confirmed by comparing the PL map of the same device before and after printing (see Figure S1, Supporting Information). A typical spectrum is presented in Figure 2B and shows a cavity resonance with a Q of about 7000 for the ground mode. For devices at the low energy tail of the QD ensemble, the Q increases to about 10 000. This is comparable to Q-factors of e-beam written cavities in the same wafer as shown in our previous work,[3] indicating that absorption in the III–V material may be the limiting factor. A PL map, shown in Figure 2B, demonstrates the localized cavity mode, which is estimated to have a small modal volume of about 2 $(\lambda/n)^3$ (according to numerical simulations incorporating the truncated Gaussian profile of the strip). Therefore, a strong optical confinement is achieved despite the small refractive index of the organic material deposited.

Attractive features of FlIJ printing on a PhC template can be seen in the AFM image of Figure 2A. The strip, typically about 2 μm wide on the bare GaAs substrate, narrows down across the PhC due to the presence of the air holes, resulting in an improved lateral resolution and minimal scalloping, such as found when printing on pore-structured films.[25] It is noteworthy that FlIJ printing inherently leads to the desired feature size.[14] In addition, FlIJ printing and a suitably formulated SPO:PMMA ink give strips with sub-100 nm thickness with no difficulty. By contrast, spin coating for example, is strongly affected by dewetting issues. Sub-100 nm thickness values are important to limit losses caused by the additional layer.[14] Furthermore, PhC cavities are usually designed by adiabatic changes of the lattice or average refractive index in order to reduce losses from radiative scattering.[26] Such desirable feature is here provided by the Gaussian profile of FlIJ printed strip.

The level of control of this fabrication method can be assessed from the ability to tune the resonances of the printed cavity by varying the strip thickness. A set of nominally identical PhC waveguides were fabricated with a different number of overlaid printer passes. The strip thickness can be increased from about 5 to 15 nm per pass depending on ink formulation and printing parameters, with little change in the strip width (see inset of Figure 2A). This allows the tuning of the cavity resonance without significant increase in the optical mode volume. Figure 2C compiles a set of PL spectra obtained from these devices. The spectra show a clear red shift of the cavity modes as a function of the number of overlaid printer passes, as expected with an increase in strip thickness (see Figure S2A–C, Supporting Information). The same printing process repeated on a fresh set of PhC waveguides results in an average tunability of the optical modes of about 1 nm per pass with a standard deviation in the absolute wavelength of about 0.5 nm (see Figure 2D). Such fine tuning of the mode wavelength requires 1 nm precision on the position of the air-holes when defining a PhC cavity of a similar type by e-beam lithography.[27] In addition, a 1 nm variation in the mode wavelength of nominally identical e-beam defined cavities is usual,[28,29] thus showing the good reproducibility of the inkjet-printed cavities. Here the small local perturbation of the PhC lattice is made possible by the deposition of femtoliter droplets of a low-refractive-index material on a high-refractive-index substrate where most of the optical mode energy is confined. This makes this cavity system robust to nonuniformity in the printing process. The small perturbation also contributes to a relatively small number of modes, which can be supported by the cavity.[30] In addition, single-mode cavities of interest for applications in lasing can be obtained by a single or two overlaid passes. The Q of the printed cavities is independent of the number of passes as seen in Figure 2E and is therefore essentially limited by the quantum dot absorption, not the strip thickness. All devices exhibit a high Q, typically between 6000 and 7000. Simulations show that $Q > 10^5$ can be indeed achieved with modal volume only twice the cubic wavelength for 40 nm thick strips (see Figure S2D, Supporting Information).

The scalability and versatility of this printing approach was further assessed by the fabrication of evanescently coupled identical cavities, or photonic molecules,[31] which have recently found remarkable applications in quantum optics and lasing.[32,33] Photonic molecules constitute a powerful benchmark for a nanophotonics technology due to their remarkable sensitivity to fabrication imperfections. In fact, while the coupling of two nominally identical cavities results in a mode splitting proportional to the coupling strength, fabrication imperfections produce detuning that can lead to an uncoupled system.[28] To fabricate a photonic molecule with our technology, a pair of strips are printed side by side, as shown in **Figure 3**A, on a set of nominally identical PhC waveguides. The separation of the strips is varied in steps of 0.5 μm. Results are presented for two overlaid printer passes, with strip thickness of about 20 nm. For a single strip, this gives single mode cavities as shown in Figure 3B. Figure 3C shows a typical spectrum of two strongly coupled cavities with printed strips separated by 3 μm. The presence of two peaks is not a sufficient proof by itself of two coupled cavities, as this could simply be the result of detuning. However, the PL map of the coupled modes in Figure 3D shows two clearly distinguishable, spatially delocalized supermodes. The mode profiles are a result of the convolution of the symmetric and antisymmetric supermodes (see Figure S3, Supporting Information) and the resolution function of the PL system. More closely spaced cavities give increased

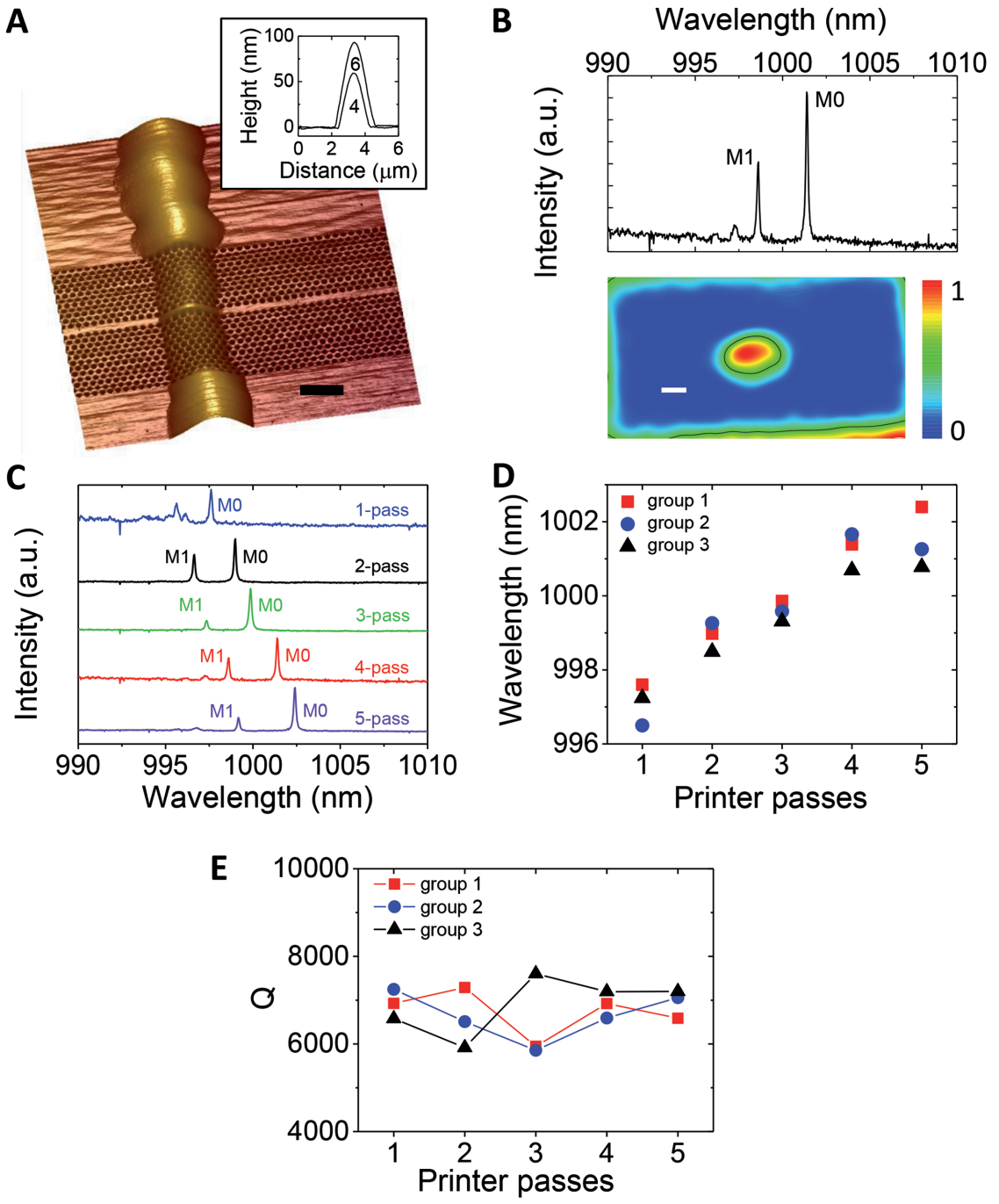

Figure 2. Nanocavity printed as a single strip across a PhC waveguide with structurally tunable cavity resonance. A) AFM image of a printed strip on a PhC (scale bar = 1 μm). Inset: cross-sectional height profile of the strip along the PhC waveguide resulting from four and six overlaid passes giving a truncated Gaussian profile with full-width half-maximum (FWHM) of 1.2 and 1.4 μm, respectively. B) PL spectra (top) of a cavity obtained from four overlaid printer passes on a PhC waveguide with 245 nm lattice, about 115 nm hole diameter and about 12 μm length showing the ground mode M0 and first excited state M1 of the cavity. (Bottom) PL Intensity mapping of the ground mode showing the rectangular footprint of the PhC template and the localized mode, with an estimated FWHM given by the black contour line (scale bar = 1 μm). C) Set of PL spectra of the printed cavity showing tunability of the ground mode M0 and first excited state M1 as a function of the number of overlaid passes. D,E) Wavelength (D) and *Q*-factor (E) of the ground mode as a function of the number of passes obtained from three nominally identical groups of five PhC waveguides.

spectral splitting consistent with an increase in the coupling strength, as shown in Figure 3E. For all double cavities with a separation of less than 3 μm, evidence of strong evanescent coupling is found in the PL maps. By contrast, most devices with larger separations are uncoupled (see Figure 3E). Beyond 3 μm, the splitting becomes dominated by cavity detuning.

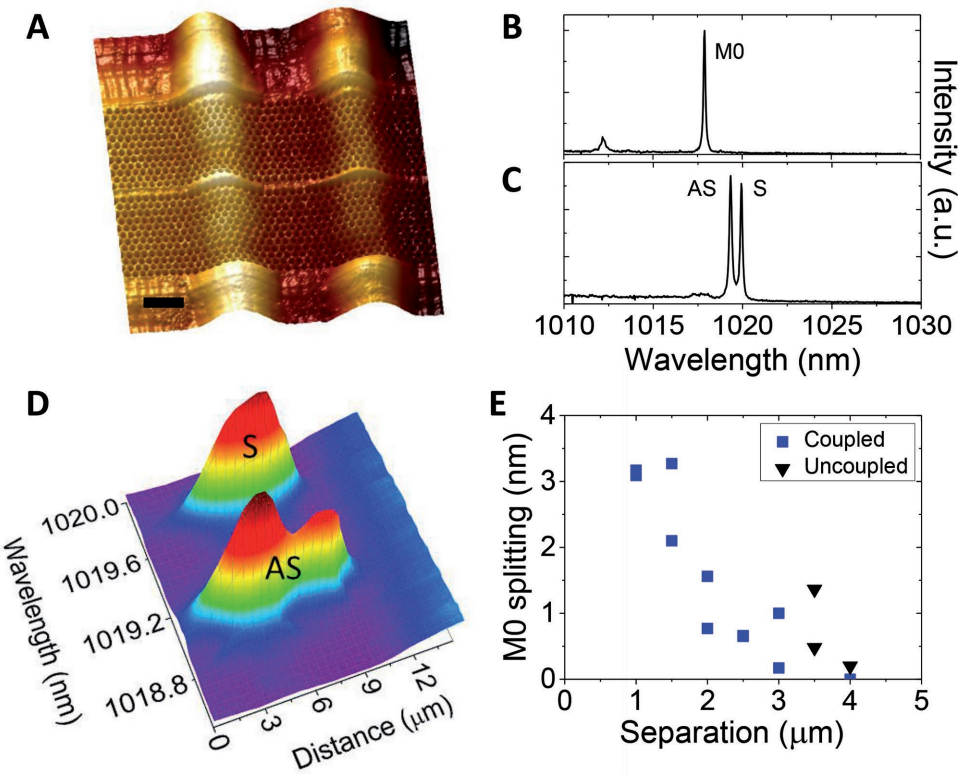

Figure 3. Printed photonic molecule with controllable energy splitting on a uniform PhC waveguide. A) AFM image showing an example of photonic molecule formed from two nominally identical printed strips on top of a uniform PhC waveguide (scale bar = 1 μm). B) PL spectra from a cavity fabricated from a single strip with two overlaid passes on a PhC waveguide. The cavity supports a single mode M0. C) PL spectra from a photonic molecule fabricated from two identical printed strips with two overlaid passes separated by 3 μm on a PhC waveguide with 245 nm lattice and about 105 nm hole diameter. The ground mode M0 in B has been split into a low energy symmetric supermode (S) and higher energy antisymmetric supermode (AS). D) PL spectra of the photonic molecule but collected along the PhC waveguide showing the mode profile of the supermodes overlapping both strips. E) Mode splitting of the photonic molecule as a function of the separation between the two printed strips.

Overall, it is shown that the coupling strength of PhC photonic molecules can be controlled using FlIJ printing simply by changing the separation of the printed strip cavities, thus overcoming limitations imposed by the discrete photonic lattice.[34]

To demonstrate direct writing of a nanocavity, we explored the creation of cavities using a blank PhC template (without any waveguide). So far, related experimental demonstrations have involved selective infiltration of PhC air-holes with a low-refractive-index fluid using a needle contacting the hole sidewall, and have opened exciting prospects for making rewritable photonic circuits[35,36] and for applications in particle sensing[37,38] or quantum optics.[39] The microfluidic technique provides great control of the cavity creation but requires the use of complex alignment procedure and of a PhC template with large hole size, restricting the achievable Q. Here we demonstrate that cavities can be created by surface deposition of a low-refractive-index material on a blank PhC template without requirement for infiltration. A single droplet is printed on top of a blank PhC forming a dot-like structure with diameter in the region of 1 μm and thickness of about 50 nm, as shown in **Figure 4**A. The rapid solvent evaporation allowed by FlIJ printing again gives structures with a convex profile, consistently with the absence of coffee ring effect. In contrast to the waveguide cavities, the organic dot hosts a number of spectrally close and spatially confined modes, as shown in Figure 4B. Numerical results shown in Figure 4C, obtained using a freely available software package,[40] confirm the creation of an optical cavity by surface deposition of a low-refractive-index material. Like the fluid filled cavity,[38] the electric field of the dot cavity mode is concentrated inside the air holes, since the dot locally red shifts the airband edge of the PhC into the photonic bandgap to create confined modes. It is noteworthy that here the ground mode extends along the Γ-K direction of the lattice, as similarly found elsewhere when there is a small local increase in the refractive index of the material.[37] Printed dots with thickness in the range of 40 to 60 nm and diameter between 1.5 and 2.5 μm give a variation of the ground wavelength mode of ±1 nm and a Q between 5000 and 6000 as seen in Figure 4D. To the best of our knowledge, this constitutes the first conceptual and experimental demonstration of cavities realized by surface deposition on a blank PhC. The Q is limited here by in-plane losses due to the small local shift of the band edge introduced by the thin dot. This is however not a fundamental limitation, as $Q > 10^5$ with same PhC size can be theoretically achieved by adjusting the design of the PhC slab template.

The surface deposition method was explored further, with the aim of reducing the performance variability found in single droplet devices. Here the design consists of two intersecting strips. At the intersection, the thickness is greater than the rest of the strips, thus emulating a printed dot as shown by

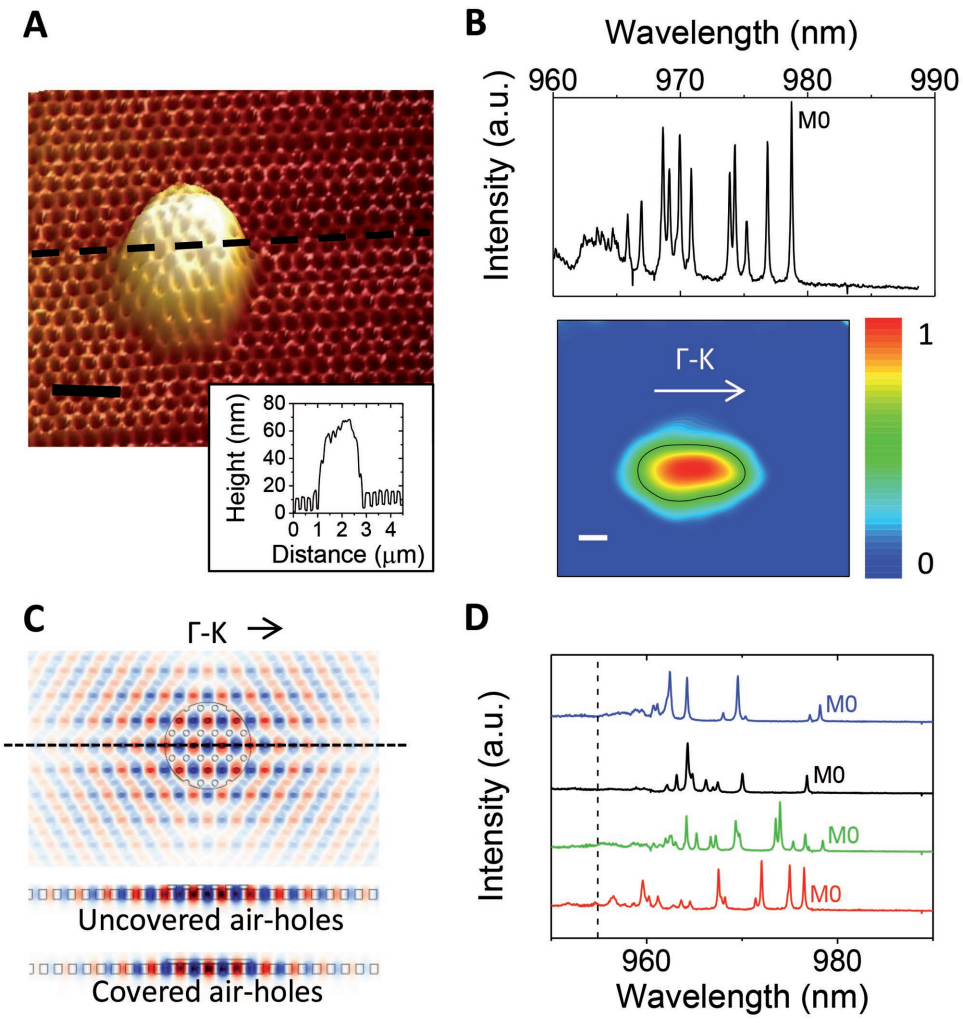

Figure 4. Printed nanocavity from a single droplet on a blank PhC template. A) AFM image showing an example of a printed dot (top) about 1.5 μm in diameter and about 50 nm thick on a blank PhC (scale bar = 1 μm). The cross-sectional height profile along the dashed line is shown below. B) PL spectra (top) of a cavity obtained from a single droplet on a blank PhC with 255 nm lattice, about 110 nm hole diameter showing the ground mode M0 of the cavity. (Bottom) PL Intensity mapping of the ground mode. The black contour indicates the estimated FWHM of the mode (scale bar = 1 μm). C) Calculated *Ey* electric field distribution of the ground mode considering a circular dot (≈50 nm thick) deposited on top of a blank PhC membrane. The cross-sectional profile of the mode through the dashed line is shown below considering the cases of uncovered air-holes (perforated dot) or covered air-holes. D) Set of PL spectra of the cavity for nominally identical printed dots with the same PhC parameters as in (B). The dashed line indicates the calculated wavelength of the air-band edge of the blank PhC.

the atomic force microscopy (AFM) scan of **Figure 5**A. A video of the printing process for this specific device is shown in the Supporting Information. This cavity supports fewer modes than the dot cavity, but with slightly lower *Q* (between 4000 and 5000) as seen in Figure 5B. Like the dot cavity, this cavity generates modes energetically close to the air-band edge of the PhC with field components concentrating in the air holes, as shown numerically in Figure 5C. It is believed that the smaller number of supported modes here is due to the small average index contrast between the dot and the strips resulting in more extended modes along the Γ-K direction of the lattice. However, due to the higher degree of structural control offered by printed strips, this design opens the possibility of tuning the mode resonances by changing the number of overlaid printer passes, as shown in Figure 5D. Note that in order to maintain high-*Q* cavities the number of passes along the Γ-K direction has to differ by one pass at most from the number of passes along the Γ-M direction (see Figure S4, Supporting Information). A tuning of about 3 nm per printer pass without degradation of the *Q* can be obtained thus opening promising avenues in tailoring the emission of cavities printed on demand on a blank PhC.

In conclusion, this work introduces a new fabrication method for nanophotonic cavities based on rapidly developing inkjet-printing technology. We have demonstrated femtoliter inkjet printing on a 2D PhC template, and the creation of reproducible and structurally tunable high-*Q*-cavities with small modal volumes.

A particular attractive feature of this bottom-up fabrication approach is the ability to fine-tune to the sub-10 nm level the thickness of the material deposited on the PhC, as achieved here by controlling the number of printer passes. This means that, in principle, a combination of materials could be stacked up,

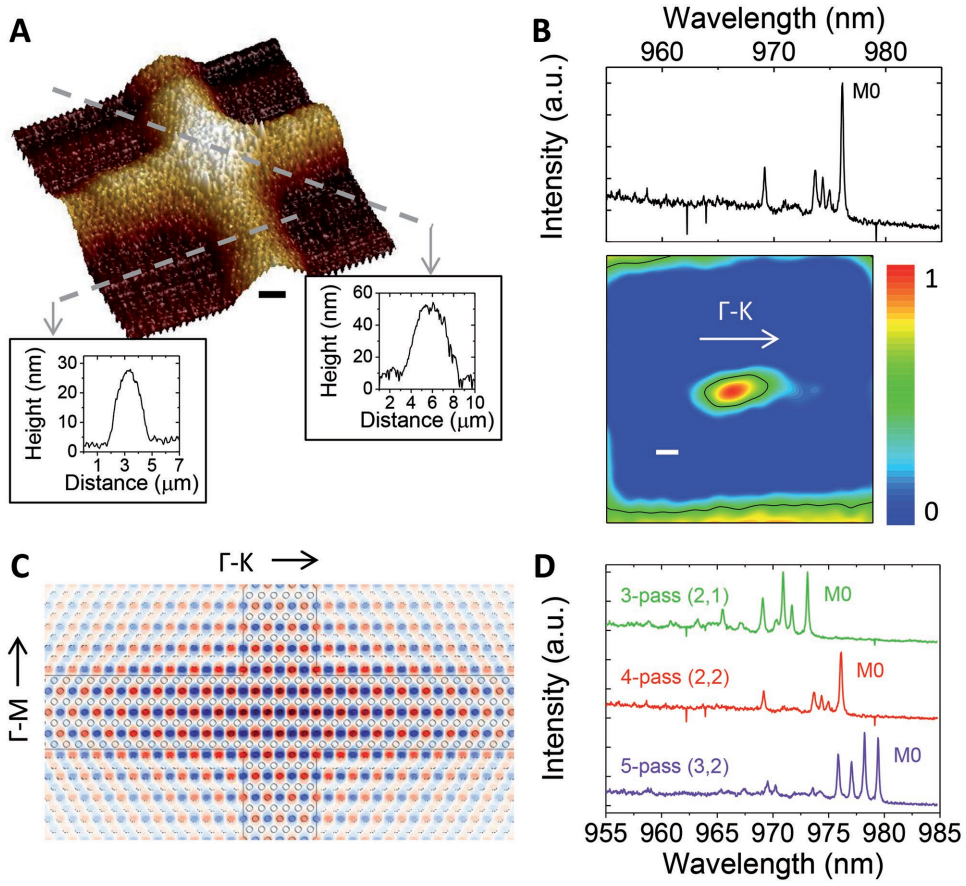

Figure 5. Printed nanocavity with structurally tunable resonant wavelength from two crossed strips on a blank PhC. A) AFM image showing an example of printed crossed strips on a blank PhC with two overlaid printer passes for each strip (scale bar = 1 μm). The cross-sectional height profile of the intersection is shown below. B) PL spectra (top) of a cavity obtained from a single droplet on a blank PhC with same parameters as for the printed dot cavity showing the ground mode M0. (Bottom) PL Intensity mapping of the ground mode. The black contour indicates the estimated FWHM of the mode (scale bar = 1 μm). C) Calculated *Ey* electric field distribution of the ground mode of the crossed strips cavity by 3D FDTD considering a strip 25 nm thick and 50 nm thick at the intersection. D) Set of PL spectra of the printed crossed strips cavity showing tunability of the ground mode M0 as a function of the number of total overlaid passes at the intersection of the strips. The first number in the bracket indicates the number of overlaid passes for the strip in the Γ-K direction, the second number in the Γ-M direction.

self-aligned, and coupled to the cavity evanescent field located near the PhC surface. This provides a tool for study of light–matter interactions, such as strong-coupling, lasing, and single photon emission in a wide range of solution-processable soft,[41] and nanomaterials, such as 2D materials[42] and quantum dots.[43,44]

One could then envisage using a generic 2D PhC template mass-produced by deep UV lithography.[12,13] This enables the exploitation of high precision lithographically patterned PhC templates in small volume applications, where the simple, material independent, and on demand deposition offered by inkjet printing is used to tailor the device to a more particular application.

We also anticipate that this femtoliter printing methodology could find applications in 2D PhC-based lab-on-chip devices for molecule sensing applications.[8–11] Biomaterials have been successfully printed,[45] and combined with the small feature size obtained on the PhC (sub-2 μm) and the ability to print identical closely spaced nanocavities (as demonstrated by the photonic molecules) may enable high density array of biosensors using multiple receptor materials.

Experimental Section

Fabrication of the Photonic Crystal Template: The wafer was grown by molecular beam epitaxy. An 180 nm slab of GaAs sits on a 1 μm $Al_{0.7}Ga_{0.3}As$ sacrificial layer. A layer of InAs/GaAs quantum dot emitters centered at a wavelength of about 920 nm, and a density of ≈100 dots μm^{-2} was grown in the middle of the GaAs layer. Photonic crystals with lattice constant between 245 and 255 nm and hole size between 110 nm and 135 nm and registration markers for the printer were patterned using a 100 kV VB6 Leica e-beam machine and reactive ion etching. The photonic crystal membrane was formed by removing the $Al_{0.7}Ga_{0.3}As$ layer with HF.

Photoluminescence Measurement Set-Up: The printed sample was mounted in a He-flow cryostat cooled to about 5 K. The dots were pumped above bandgap with a 780 nm laser diode, focused to a ≈1 μm spot size using a 100× microscope objective (numerical aperture 0.5). The emission was analyzed by a 0.55 m spectrometer with 1200 L mm^{-1} grating and a LN_2 cooled CCD camera. The optical modes were spatially mapped using the microscope in a confocal configuration and a piezoelectric *xyz* nanopositioning stage.

Synthesis of the Ink: The ink was obtained by dissolving PMMA (average $M_w \approx 120$ kDa) and 1,3,3-trimethylindolinonaphthospirooxazine (SPO) in 1,2-dichlorobenzene (DCB). Dissolution was achieved by

stirring the mixture at room temperature. For printed strips, the desired ink composition was achieved by dissolving 27.3 mg of SPO and 2.73 mg of PMMA in 1 mL of DCB. For printed dots, a different ink composition was used: 3.9 mg of SPO and 0.39 mg of PMMA were added for every milliliter of DCB.

Printing: Printing was carried out with a Super Inkjet Printer SIJ-S050[19] and Superfine nozzles (SIJTechnology Inc.). The photonic crystal template was mounted on the printer piezoelectric *xy* positioning stage. The printer nozzle was aligned to the templates using registration markers on the sample and the printer CCD camera. The nozzle motion and droplet ejection mechanism were controlled by a text-based pattern description language developed by SIJTechnology.

In the case of strips and crosses, jetting was achieved by applying a 100 Hz square waveform of 300–500 V amplitude superimposed on 300–400 V DC bias. The nozzle speed relative to the substrate was in the region of 0.1 mm s^{-1}. Dots were obtained by jetting from a 1 Hz square waveform of 230–250 V amplitude and 170 V DC bias, with a holding time in the region of 200 ms. Following printing, a short annealing step (about 1 h) in a low temperature oven (about 60 °C) was sufficient to remove all solvent from the printed ink to give air-stable features.

Supporting Information

Supporting Information is available from the Wiley Online Library or from the author.

Acknowledgements

F.S.F.B. and V.P. contributed equally to this work. Part of this work was performed using the Darwin Supercomputer of the University of Cambridge High Performance Computing Service (http://www.hpc.cam.ac.uk/), provided by Dell Inc. using Strategic Research Infrastructure Funding from the Higher Education Funding Council for England and funding from the Science and Technology Facilities Council. V.P. gratefully acknowledges financial support from the United Kingdom Engineering and Physical Sciences Research Council (EPSRC) through the Centre for Innovative Manufacturing in Large Area Electronics (CIMLAE, program grant EP/K03099X/1) and the project Integration of Printed Electronics with Silicon for Smart sensor systems (iPESS). V.P. also acknowledges financial support from the Priority Academic Program Development of Jiangsu Higher Education Institutions (PAPD) and the Collaborative Innovation Center of Suzhou Nano Science and Technology. The authors are thankful to Kai Xia for the help with the illustrations. F.S.F.B. is thankful to Prof. Robert Taylor for helpful discussions concerning the optical set-up.

Conflict of Interest

The authors declare no conflict of interest.

Keywords

femtoliter inkjet printing, hybrid optical nanocavities, photonic crystals, photonic molecules

Received: August 6, 2017
Published online: October 24, 2017

[1] T. Yoshie, A. Scherer, J. Hendrickson, G. Khitrova, H. M. Gibbs, G. Rupper, C. Ell, O. B. Shchekin, D. G. Deppe, *Nature* **2004**, *432*, 200.
[2] K. Hennessy, A. Badolato, M. Winger, D. Gerace, M. Atatüre, S. Gulde, S. Fält, E. L. Hu, A. Imamoğlu, *Nature* **2007**, *445*, 896.
[3] F. S. F. Brossard, X. L. Xu, D. A. Williams, M. Hadjipanayi, M. Hugues, M. Hopkinson, X. Wang, R. A. Taylor, *Appl. Phys. Lett.* **2010**, *97*, 111101.
[4] D. Englund, D. Fattal, E. Waks, G. Solomon, B. Zhang, T. Nakaoka, Y. Arakawa, Y. Yamamoto, J. Vučkovic, *Phys. Rev. Lett.* **2005**, *95*, 13904.
[5] W. H. Chang, W. Y. Chen, H. S. Chang, T. P. Hsieh, J. I. Chyi, T. M. Hsu, *Phys. Rev. Lett.* **2006**, *96*, 117401.
[6] M. Lončar, T. Yoshie, A. Scherer, P. Gogna, Y. Qiu, *Appl. Phys. Lett.* **2002**, *81*, 2680.
[7] B. Ellis, M. A. Mayer, G. Shambat, T. Sarmiento, J. Harris, E. E. Haller, J. Vučkovic, *Nat. Photonics* **2011**, *5*, 297.
[8] M. R. Lee, P. M. Fauchet, *Opt. Express* **2007**, *15*, 4530.
[9] A. Di Falco, L. O'Faolain, T. F. Krauss, *Appl. Phys. Lett.* **2009**, *94*, 063503.
[10] J. E. Baker, R. Sriram, B. L. Miller, *Lab Chip* **2015**, *15*, 971.
[11] H. Inan, M. Poyraz, F. Inci, M. A. Lifson, M. Baday, B. T. Cunningham, U. Demirci, *Chem. Soc. Rev.* **2017**, *46*, 366.
[12] K. K. Mehta, J. S. Orcutt, O. Tehar-Zahav, Z. Sternberg, R. Bafrali, R. Meade, R. J. Ram, *Sci. Rep.* **2014**, *4*, 4077.
[13] Y. Ooka, T. Tetsumoto, A. Fushimi, W. Yoshiki, T. Tanabe, *Sci. Rep.* **2015**, *5*, 11312.
[14] S. Tomljenovic-Hanic, C. M. De Sterke, M. J. Steel, B. J. Eggleton, Y. Tanaka, S. Noda, *Opt. Express* **2007**, *15*, 17248.
[15] S. Gardin, F. Bordas, X. Letartre, C. Seassal, A. Rahmani, R. Bozio, P. Viktorovitch, *Opt. Express* **2008**, *16*, 6331.
[16] M.-K. Seo, J.-H. Kang, M.-K. Kim, B.-H. Ahn, J.-Y. Kim, K.-Y. Jeong, H.-G. Park, Y.-H. Lee, *Opt. Express* **2009**, *17*, 6790.
[17] S. Prorok, A. Petrov, M. Eich, J. Luo, A. K. Jen, *Appl. Phys. Lett.* **2013**, *103*, 261112.
[18] J.-U. Park, M. Hardy, S. J. Kang, K. Barton, K. Adair, D. kishore Mukhopadhyay, C. Y. Lee, M. S. Strano, A. G. Alleyne, J. G. Georgiadis, P. M. Ferreira, J. A. Rogers, *Nat. Mater.* **2007**, *6*, 782.
[19] K. Murata, K. Masuda, *Convert. e-Print, SIJTechnology Inc.* **2011**, 74, http://www.sijtechnology.com/en/.
[20] P. Galliker, J. Schneider, H. Eghlidi, S. Kress, V. Sandoghdar, D. Poulikakos, *Nat. Commun.* **2012**, *3*, 890.
[21] Z. Cui, C. Zhou, Z. Chen, C. Ma, J. Zhao, W. Su, *Printed Electronics: Materials, Technologies and Applications*, Wiley, Singapore **2016**.
[22] R. D. Deegan, O. Bakajin, T. F. Dupont, G. Huber, S. R. Nagel, T. A. Witten, *Nature* **1997**, *389*, 827.
[23] J. X. Wang, L. B. Wang, Y. L. Song, L. Jiang, *J. Mater. Chem. C* **2013**, *1*, 6048.
[24] C. Zhang, C. Zou, Y. Zhao, C. Dong, C. Wei, H. Wang, Y. Liu, G.-C. Guo, J. Yao, Y. S. Zhao, *Sci. Adv.* **2015**, *1*, e1500257.
[25] C. Kim, M. Nogi, K. Suganuma, Y. Yamato, *ACS Appl. Mater. Interfaces* **2012**, *4*, 2168.
[26] Y. Akahane, T. Asano, B. Song, S. Noda, *Nature* **2003**, *425*, 944.
[27] E. Kuramochi, M. Notomi, S. Mitsugi, A. Shinya, T. Tanabe, T. Watanabe, *Appl. Phys. Lett.* **2006**, *88*, 041112.
[28] F. S. F. Brossard, B. P. L. Reid, C. C. S. Chan, X. L. Xu, J. P. Griffiths, D. A. Williams, R. Murray, R. A. Taylor, *Opt. Express* **2013**, *21*, 16934.
[29] L. Ramunno, S. Hughes, *Phys. Rev. B: Condens. Matter Mater. Phys.* **2009**, *79*, 1.
[30] A. Mock, L. Lu, E. H. Hwang, J. O'Brien, P. D. Dapkus, *IEEE J. Sel. Top. Quantum Electron.* **2009**, *15*, 892.
[31] M. Bayer, T. Gutbrod, J. Reithmaier, A. Forchel, T. Reinecke, P. Knipp, A. Dremin, V. Kulakovskii, *Phys. Rev. Lett.* **1998**, *81*, 2582.
[32] R. Bose, T. Cai, K. Choudhury, G. Solomon, E. Waks, *Nat. Photonics* **2014**, *8*, 858.
[33] P. Hamel, S. Haddadi, F. Raineri, P. Monnier, G. Beaudoin, I. Sagnes, A. Levenson, A. M. Yacomotti, *Nat. Photonics* **2015**, *9*, 311.

[34] A. R. A. Chalcraft, S. Lam, B. D. Jones, D. Szymanski, R. Oulton, A. C. T. Thijssen, M. S. Skolnick, D. M. Whittaker, T. F. Krauss, A. M. Fox, *Opt. Express* **2011**, *19*, 5670.
[35] F. Intonti, S. Vignolini, V. Türck, M. Colocci, P. Bettotti, L. Pavesi, S. L. Schweizer, R. Wehrspohn, D. Wiersma, *Appl. Phys. Lett.* **2006**, *89*, 211117.
[36] C. Grillet, C. Monat, C. L. Smith, M. W. Lee, S. Tomljenovic-Hanic, C. Karnutsch, B. J. Eggleton, *Laser Photonics Rev.* **2010**, *4*, 192.
[37] S. Tomljenovic-Hanic, C. M. de Sterke, *Opt. Express* **2010**, *18*, 21397.
[38] S. Tomljenovic-Hanic, C. M. de Sterke, *Sensors* **2013**, *13*, 3262.
[39] S. Tomljenovic-Hanic, A. D. Greentree, B. C. Gibson, T. J. Karle, S. Prawer, *Opt. Express* **2011**, *19*, 22219.
[40] A. F. Oskooi, D. Roundy, M. Ibanescu, P. Bermel, J. D. Joannopoulos, S. G. Johnson, *Comput. Phys. Commun.* **2010**, *181*, 687.
[41] K. Kim, G. Kim, B. R. Lee, S. Ji, S.-Y. Kim, B. W. An, M. H. Song, J.-U. Park, *Nanoscale* **2015**, *7*, 13410.
[42] B. W. An, K. Kim, M. Kim, S.-Y. Kim, S.-H. Hur, J.-U. Park, *Small* **2015**, *11*, 2263.
[43] S. J. P. Kress, P. Richner, S. V. Jayanti, P. Galliker, D. K. Kim, D. Poulikakos, D. J. Norris, *Nano Lett.* **2014**, *14*, 5827.
[44] B. H. Kim, M. S. Onses, J. Bin Lim, S. Nam, N. Oh, H. Kim, K. J. Yu, J. W. Lee, J. H. Kim, S. K. Kang, C. H. Lee, J. Lee, J. H. Shin, N. H. Kim, C. Leal, M. Shim, J. A. Rogers, *Nano Lett.* **2015**, *15*, 969.
[45] J. U. Park, J. H. Lee, U. Paik, Y. Lu, J. A. Rogers, *Nano Lett.* **2008**, *8*, 4210.